

Collaborative Large Language Model Inference via Resource-Aware Parallel Speculative Decoding

Jungyeon Koh

Department of Electrical Engineering

POSTECH

Pohang, Republic of Korea

jungyeon.koh@postech.ac.kr

Hyun Jong Yang

Department of Electrical and Computer Engineering

Seoul National University

Seoul, Republic of Korea

hgyang@snu.ac.kr

Abstract—The growing demand for on-device large language model (LLM) inference highlights the need for efficient mobile edge computing (MEC) solutions, especially in resource-constrained settings. Speculative decoding offers a promising solution by partitioning token generation between a lightweight draft model on mobile devices and a powerful target model on edge servers, but suffers from communication overhead and asynchronous delays. This paper is the first to propose a unified framework that jointly optimizes user association and resource allocation (UARA) to support efficient parallel speculative decoding. We solve the UARA problem using a multi-agent deep reinforcement learning algorithm. To evaluate our approach under realistic conditions, we conduct experiments using the Sionna simulator. Results show that our method achieves up to 28.0% and an average of 23.7% reduction in end-to-end latency without compromising inference accuracy, enabling scalable and low-latency LLM services in MEC systems.

Index Terms—Speculative Decoding, Collaborative Inference, User Association, Resource Allocation, Multi-Agent Deep Reinforcement Learning

I. INTRODUCTION

The rising demand for on-device large language models (LLMs) has imposed a significant computational burden on mobile devices, especially in developing countries with limited hardware and infrastructure. This challenge has spurred research interest in the efficient deployment of mobile edge computing (MEC) to assist resource-constrained environments. Although conventional approaches—on-device and cloud-based inference—offer baseline support, both face critical limitations. On-device LLM inference is compute- and memory-intensive; for example, running a Llama2-7B model requires approximately 28 GB of memory, far beyond the capacity of most mobile devices [1]. Even high-end smartphones often suffer from battery drain and degraded quality of experience (QoE). Meanwhile, cloud-based solutions like ChatGPT and Gemini introduce latency, bandwidth costs, and privacy concerns.

This work was supported by the IITP(Institute of Information & Communications Technology Planning & Evaluation)-ITRC(Information Technology Research Center) grant funded by the Korea government(Ministry of Science and ICT)(IITP-2025-2021-0-02048) and Institute of Information & communications Technology Planning & Evaluation (IITP) grant funded by the Korea government(MSIT) (IITP-2025-2021-0-00161, 6G MIMO System Research) (IITP-2025-RS-2024-00404972, Development of 5G-A vRAN Research Platform).

To address these challenges, mobile-edge collaborative inference has emerged as a promising solution. By distributing computation between mobile devices and nearby edge servers, this approach enables real-time LLM inference by integrating edge computing, model optimization, and mobile hardware. Existing collaborative methods [2], [3] focus primarily on partitioning deep neural networks (DNNs) and offloading subsequent computation stages to edge servers. For example, [2] proposes spatially tiling the computation graph to enable independent execution among tiles, which works well for convolutional neural networks. However, such methods are ill-suited for autoregressive language models, where sequential token dependencies make partitioning inherently challenging.

To mitigate the inefficiencies of autoregressive generation, speculative decoding [4], [5] employs a lightweight *draft* model on the mobile device and a more powerful *target* model on the edge server. The draft model generates draft tokens with minimal computational cost, while the target model verifies and refines them in batches. This significantly reduces computational overhead while preserving inference accuracy. However, speculative decoding still faces latency issues, mainly due to asynchronous executions. As sequence lengths grow, a *mutual waiting problem* arises—the target model remains idle while awaiting tokens from the draft model, and the draft model similarly stops during target-side verification. This inefficiency hinders the overall performance gain and suggests opportunities for further optimization.

To address this, [6] proposes parallel speculative decoding (PSD), which overlaps the drafting and verifying phases to reduce overall processing time. However, PSD introduces additional communication overhead, limiting its feasibility in mobile-edge collaborative inference. Motivated by these challenges, this paper highlights the need for intelligent user association and resource allocation (UARA) strategies to fully exploit the benefits of speculative decoding in MEC systems. Furthermore, we incorporate device-level constraints—such as remaining battery life—into UARA decisions for sustainable and efficient operations, given the heavy reliance of speculative decoding on mobile-side computation.

Building on these insights, we propose a novel UARA optimization framework for efficient parallel speculative decoding. Our approach addresses user association via Two-

Phase Matching-based Association (TMA) [7] and applies a Multi-Agent Soft Actor-Critic (MASAC) [8] network to optimize resource allocation. To the best of our knowledge, this is the first work to jointly optimize UARA problem for speculative decoding in MEC environments.

Our key contributions are summarized as follows:

- **Unified UARA strategy for speculative decoding:** We propose the first unified framework that jointly optimizes UARA problem to enable low-latency LLM inference via parallel speculative decoding.
- **Joint optimization problem formulation:** We identify synchronization between mobile-side computation and up-link communication as critical to fully utilizing parallel speculative decoding. To this end, we formulate a mixed-integer, non-convex optimization problem, which is addressed using our proposed MADRL-based solution.
- **Realistic simulation using Sionna:** We use the Sionna [9] simulator to conduct realistic experiments based on advanced ray tracing and geo-located wireless channels. This allows us to closely mimic real-world MEC systems with dynamic user mobility and varying channel conditions.
- **Performance evaluation and analysis:** We implement our UARA scheme on Sionna-based setups with a diverse set of mobile devices and edge servers. Numerical results show up to 28.0% and an average of 23.7% reduction in end-to-end latency without compromising inference accuracy, thus validating the practicality of our approach in realistic MEC settings.

II. PRELIMINARIES

A. Iterative LLM Inference

The LLM inference process is inherently iterative and typically consists of two distinct phases: *prompt processing (prefill)* and *autoregressive generation*. These phases differ significantly in their computational and memory characteristics.

- **Prompt Processing:** In this phase, the model processes the initial sequence $\mathbf{x} = (x_1, \dots, x_n)$ to generate the first new token x_{n+1} by computing the conditional probability $P(x_{n+1}|x_1, \dots, x_n)$. This step involves generating key-value (KV) pairs for all input tokens, which are cached for use in subsequent decoding steps. Since the entire input sequence is available upfront, the phase can be easily accelerated on modern hardware. Thus, prefill is typically compute-bound and exhibits high throughput.
- **Autoregressive Generation:** In the generation phase, the model produces one token at a time, with each token conditioned on all previously generated tokens. Generation continues until a stopping criterion is met, such as generating an end-of-sequence (EOS) token or reaching a specified maximum token limit. Unlike the prefill phase, this phase is primarily memory-bound since frequent memory access dominates latency. Consequently, token throughput in this phase is significantly lower, posing a major bottleneck in real-time LLM inference.

B. Speculative Decoding

Parallelizing autoregressive generation in LLMs is challenging due to its inherent sequential dependency, where each token depends on all previous ones. Speculative decoding mitigates this by adopting a *draft-then-verify* strategy using a lightweight *draft* model for fast token generation and a more accurate *target* model for verification. By allowing the draft model to generate likely tokens quickly and delegating uncertain ones to the target model, this approach reduces sequential computation and expedites inference.

In speculative decoding, the draft model M_q and the target model M_p operate with a fixed hyperparameter γ , which specifies the draft length—the number of tokens generated by the draft model per iteration. The process begins with M_q generating γ draft tokens $(x_1, x_2, \dots, x_\gamma)$ along with their corresponding logits $(q_1, q_2, \dots, q_\gamma)$. The target model M_p then processes the concatenated sequence $(x, x_1, \dots, x_\gamma)$ and produces logits $(p_1, p_2, \dots, p_{\gamma+1})$. Each draft token x_i is verified with the acceptance rate α_i defined as

$$\alpha_i = \begin{cases} 1 & p_i[x_i] \geq q_i[x_i] \\ \frac{p_i[x_i]}{q_i[x_i]} & p_i[x_i] < q_i[x_i] \end{cases} \quad (1)$$

If a draft token x_i is rejected, it is resampled from $p_i - q_i$; otherwise, the process proceeds to generate $x_{\gamma+1}$ via $p_{\gamma+1}$. This method ensures that each step generates at most $\gamma + 1$ tokens, thereby speeding up the generation process. However, we eliminate resampling and directly regenerate rejected tokens using the target model, reducing communication overhead from transmitting full logits q_i .

While most prior works focus mainly on reducing computation latency—via compact or draft-free models [10]–[12] or improved alignment between draft and target distributions [13], [14]—these are often limited to single-device setups. Only few recent efforts have explored speculative decoding in MEC contexts [15], [16]. However, they often overlook the interplay between computation and communication, lacking practical and feasible strategies for real-world deployments.

C. Parallel Speculative Decoding

We introduce a parallel speculative decoding framework, inspired by recent work in [6], to enable synchronized execution of draft and target models. Unlike conventional speculative decoding, which alternates between draft and verify stages, PSD proposes dynamic scheduling—*pre-verify* and *post-verify*—for concurrent execution. These strategies adaptively switch based on token verification outcomes, effectively overlapping computation and reducing idle time. Figure 1 shows the differences between conventional and parallel speculative decoding in terms of token generation behavior and execution timeline.

In the pre-verify phase, the target model M_p computes logits $M_p(\mathbf{x})$ while the draft model generates a batch of tokens. If the first token is rejected, the batch is discarded and a new drafting round begins immediately with the updated prefix $\mathbf{x} + (y_1)$. This enables a fast recovery from early rejections. If accepted, the process enters the post-verify phase, where the draft model

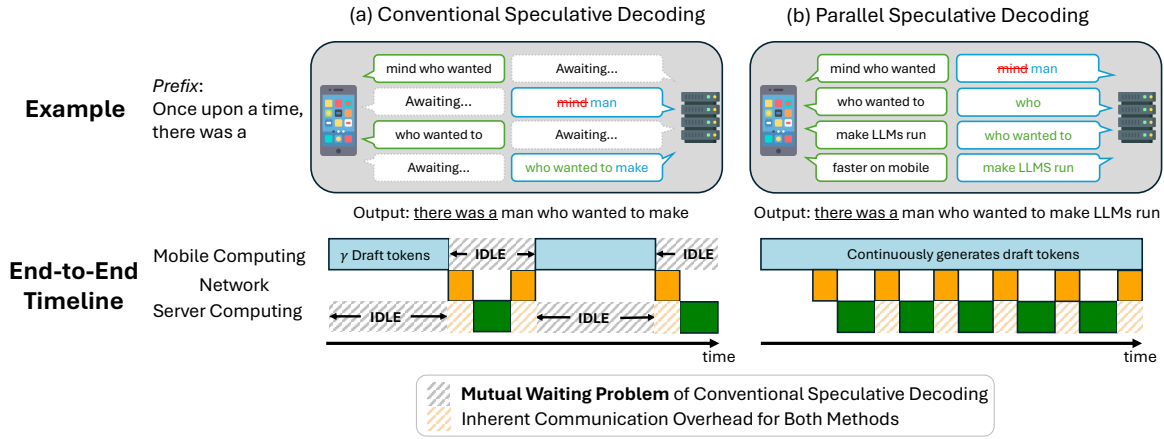


Fig. 1: Comparison of (a) conventional and (b) parallel speculative decoding. **(Top)** Example of token generation. In (a), the draft model waits for server-side verification and the target model waits for draft generation. In contrast, (b) allows continuous generation for both models, resulting in faster task completion. **(Bottom)** End-to-end timeline illustrating the interplay between mobile computation, network transmission and server computation. In (a), the sequential draft-then-verify process introduces prolonged idle time and inefficient resource utilization. In contrast, (b) reduces idle periods by enabling concurrent execution. The shaded regions in the timeline highlight the mutual waiting problem unique to the conventional approach and the inherent communication overhead present in both methods.

continues generating tokens without interruption and the target model concurrently verifies them. A rejection during this phase triggers a return to pre-verify phase.

By dynamically switching between these two phases, the PSD framework maintains uninterrupted utilization of both models and reduces idle time. However, we observe that this synchronization is fragile and can easily degrade when mobile-side computation and network latency are not properly aligned.

D. Motivating Observations

Figure 2 presents the total execution time for conventional and parallel speculative decoding under varying conditions. The key limitations of each method are summarized as follows:

- **Conventional speculative decoding** lacks adaptability across diverse prompts due to its fixed draft length γ . The optimal γ is 25 for HumanEval and 15 for DailyMail dataset. This motivates the adoption of parallel speculative decoding for adaptive and task-aware generation.
- **Parallel speculative decoding** benefits from higher bandwidth, but saturates beyond 50 Mbps, where mobile-side computation becomes the bottleneck. This underscores the need for tight synchronization between mobile computation and uplink communication.

III. SYSTEM MODEL AND PROBLEM FORMULATION

A. System Overview

Figure 3 illustrates our collaborative MEC system, which consists of M mobile devices and E edge servers. The set of mobile devices is denoted by $\mathcal{M} = \{m_1, \dots, m_M\}$, where each device may exhibit varying mobility patterns and remaining battery levels B_i . The set of edge servers is denoted by $\mathcal{E} = \{e_1, e_2, \dots, e_E\}$, equipped with varying computing resources.

To capture the effects of user mobility and time-varying channel conditions, we adopt a time-slotted model that divides

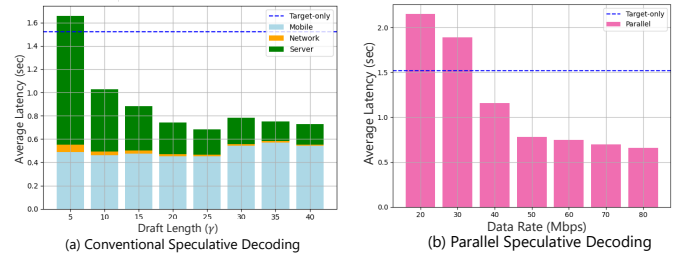


Fig. 2: Latency of (a) conventional and (b) parallel speculative decoding using HumanEval dataset. **(left)** Latency is broken down into mobile computation, network transmission and server computation for varying draft lengths. **(right)** Total latency is measured across different data rates.

the offloading period into T slots with an equal duration τ . In this quasi-static setting, channel states and device parameters are assumed constant within a slot, but may vary across slots.

We assume that each mobile device generates one task per time slot. The task generated by device m_i is represented by a tuple $\{d_i, f_i^{MD}, f_i^{ES}\}$, where d_i denotes the communication load in bits, and f_i^{MD} and f_i^{ES} are the required number of FLOPs for mobile device and edge server, respectively.

We then define the association of mobile device m_i to edge server e_j using a binary decision variable.

$$x_{ij} = \begin{cases} 1, & \text{if edge server } j \text{ serves mobile device } i, \\ 0, & \text{otherwise.} \end{cases} \quad (2)$$

Each mobile device must offload its task to exactly one edge server, with no partial offloading allowed. Accordingly, the user association variable x_{ij} is constrained by

$$\sum_{j \in \mathcal{E}} x_{ij} = 1, x_{ij} \in \{0, 1\}, \forall i \in \mathcal{M}, j \in \mathcal{E} \quad (3)$$

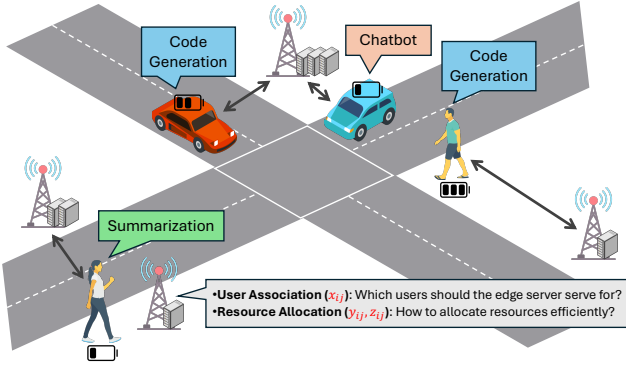


Fig. 3: Illustration of the proposed MEC system. M mobile devices, with limited battery and varying mobility, generate diverse LLM tasks. E edge servers, with varying computing capabilities, collaboratively execute these tasks. Bidirectional arrows show the collaborative nature of parallel speculative decoding. Key UARA decision variables are indicated in red.

B. Communication Model

We assume that the total network bandwidth W is equally divided among the E edge servers, such that each server e_j is allocated with $W_j = W/E$. Each server further allocates its bandwidth W_j among the mobile devices it serves. Let $y_{ij} \in [0, 1]$ denote the fraction of W_j allocated to mobile device m_i . To prevent overlapping allocations, y_{ij} is constrained by

$$\sum_{j \in \mathcal{E}} y_{ij} \leq 1, y_{ij} \in [0, 1], \forall i \in \mathcal{M}, j \in \mathcal{E} \quad (4)$$

Let h_{ij} denote the channel gain between device m_i and edge server e_j . The corresponding signal-to-noise ratio (SNR) is given by $SNR_{ij} = \frac{h_{ij}^2 P_i}{N_0}$, where P_i is the transmission power of device m_i and N_0 is the noise power spectral density.

Then, the data rate R_i of mobile device m_i is expressed as

$$R_i = \sum_{j \in \mathcal{E}} x_{ij} y_{ij} W_j \log(1 + SNR_{ij}) \quad (5)$$

C. Computing Model

Computing latency for a task requiring f_i FLOPs is calculated by dividing the task size by the available computing capacity. For remote execution, we model the delay in two phases: a *waiting phase* over k time slots of queuing delay and a *computing phase* based on the server's processing power. Since edge servers share resources across tasks, we define z_{ij} as the fraction of computing capacity allocated to the task from mobile device m_i . The resulting computing delays for local and remote execution are given by

$$\begin{cases} D_i^{\text{MD}} = \frac{f_i}{F_i^{\text{MD}}}, & \text{(local execution)} \\ D_{ij}^{\text{ES}} = k\kappa + \frac{f_i}{z_{ij} F_j^{\text{ES}}}, & \text{(remote execution)} \end{cases} \quad (6)$$

Similar to Eq. (4), the computing resource variable z_{ij} is also constrained by

$$\sum_{i \in \mathcal{M}} z_{ij} \leq 1, z_{ij} \in [0, 1], \forall i \in \mathcal{M}, j \in \mathcal{E} \quad (7)$$

D. Problem Formulation

Effective parallel speculative decoding requires synchronization between mobile computation and uplink communication overhead. Additionally, minimizing edge-side computing latency is critical for reducing end-to-end delay. To ensure sustainable operation in resource-constrained MEC settings, we further incorporate remaining battery life of mobile devices [17]. Based on these considerations, we formulate a multi-objective cost function that balances latency synchronization, remote computation delay, and energy efficiency.

Here, we define $\delta^{\text{CP}}, \delta^{\text{CM}}$ as the computing and transmission energy efficiencies, respectively. The energy consumption of mobile device m_i can then be expressed as follows.

$$\begin{cases} E_i^{\text{CP}} = \delta^{\text{CP}} f_i^{\text{MD}}, & \text{(mobile computing)} \\ E_i^{\text{CM}} = \delta^{\text{CM}} \sum_{j \in \mathcal{E}} (x_{ij} y_{ij} W_j) P_i, & \text{(uplink transmission)} \end{cases} \quad (8)$$

Then, our optimization objective \mathcal{I} can be formulated as

$$\begin{aligned} \min_{\mathbf{X}, \mathbf{Y}, \mathbf{Z}} \quad & \sum_{i \in \mathcal{M}} \sum_{j \in \mathcal{E}} x_{ij} \left(D_i^{\text{MD}} + D_{ij}^{\text{ES}} + \lambda \left\| D_i^{\text{MD}} - \frac{d_i}{R_i} \right\|_2^2 \right) \\ & + w \sum_{i \in \mathcal{M}} \frac{E_i^{\text{CP}} + E_i^{\text{CM}}}{B_i} \\ \text{s.t.} \quad & (3), (4), (7) \end{aligned} \quad (\mathcal{P}_1)$$

where λ is a penalty weight for latency synchronization, and w is a unit conversion factor normalizing energy efficiency. For clarity, we define the decision variable matrices \mathbf{X}, \mathbf{Y} and \mathbf{Z} to represent user association, bandwidth allocation, and computing resource allocation, respectively.

The primary challenge in Problem \mathcal{P}_1 lies in its formulation as a mixed-integer, non-convex optimization problem. The binary variable \mathbf{X} introduces combinatorial complexity and is further coupled with the continuous variables \mathbf{Y} and \mathbf{Z} , making the problem particularly difficult to solve.

IV. MADRL-BASED UARA SCHEME

A. Two-Phase Matching-based Association (TMA)

Two-Phase Matching-based Association (TMA) efficiently solves the user association problem through a two-phase process. In the first phase, each mobile device pre-evaluates edge servers based on channel gain to establish a favorable initial association for subsequent optimization steps. In the second phase, a matching algorithm iteratively swaps device-server pairs to minimize the objective function \mathcal{I} formulated in Problem \mathcal{P}_1 until no further improvements are possible. Compared to traditional heuristics like greedy search, matching-based methods offer faster convergence with lower complexity [18], making them suitable for dynamic MEC environments.

We present a detailed implementation of the proposed TMA scheme in Alg. 1.

B. Proposed TMA-MASAC Framework

We adopt a deep reinforcement learning (DRL) framework to address the resource allocation problem. The system state $s(t)$ includes mobile device and edge server positions, channel gain matrix \mathbf{H} , task information $\{d_i, f_i^{MD}, f_i^{ES}\}$, remaining battery level B_i for each mobile device m_i , and queuing delay k_j at each edge server e_j . The action $a(t)$ consists of uplink bandwidth allocation $\mathbf{Y}(t)$ and edge computing resource allocation $\mathbf{Z}(t)$. The reward $r(t)$ is defined as the normalized objective value, dividing \mathcal{I} by a baseline obtained from random user association and uniform resource allocation.

Specifically, we use a multi-agent soft actor-critic (MASAC) network for two reasons. First, the continuous variables \mathbf{Y} and \mathbf{Z} require a model-free, policy-gradient method. Second, SAC maximizes both the expected reward and policy entropy, encouraging explorations and enabling more robust adaptation to dynamic MEC environments.

The proposed framework consists of a policy network $\pi_\theta(a_t|s_t)$, a critic network $Q_\phi(s_t, a_t)$, and a target critic network $Q_{\bar{\phi}}(s_t, a_t)$. Introducing α as the temperature coefficient of policy entropy, MASAC optimizes the following objective

$$J(\pi) = \sum_{t=1}^T \mathbb{E}_{(s_t, a_t) \sim \pi_\theta} [r(s_t, a_t) - \alpha \log(\pi(\cdot|s_t))] \quad (9)$$

To improve sample efficiency, we adopt offline sampling by reusing historical data. Mini-batches sampled from a replay buffer are used to update the policy and critic networks, while the target critic network is softly updated, following $\bar{\phi}_i \leftarrow \xi \phi_i + (1 - \xi) \bar{\phi}_i$, where ξ denotes the soft update coefficient.

To jointly solve UARA problem, the TMA-based user association is integrated into the MASAC scheme. Fig. 4 shows the overall framework. Specifically, at each time step, the policy network outputs resource allocation decisions, after which Alg. 1 is applied to determine user association \mathbf{X} based on the updated \mathbf{Y} and \mathbf{Z} .

Algorithm 1 Two-phase Matching-based Association (TMA)

- 1: **Initialization:** Obtain the channel gain matrix \mathbf{H} between all mobile devices and edge servers.
- 2: **Phase 1:** Channel Gain-based Pre-evaluation
- 3: **for all** $m \in \mathcal{M}$ **do**
- 4: Select the edge server e with the highest gain $\mathbf{H}_{m,e}$.
- 5: Set $\mathbf{X}_{m,e} \leftarrow 1$.
- 6: **end for**
- 7: **Phase 2:** Iterative Swap-based Optimization
- 8: **while** swap pair exists **do**
- 9: **for all** $(m, e), (m', e')$ with $\mathbf{X}_{m,e} = \mathbf{X}_{m',e'} = 1$ **do**
- 10: Compute $\mathcal{I}_{(m,e),(m',e')}$ and $\mathcal{I}_{(m,e'),(m',e)}$.
- 11: **if** $\mathcal{I}_{(m,e'),(m',e)} > \mathcal{I}_{(m,e),(m',e')}$ **then**
- 12: Set $\mathbf{X}_{m,e'} \leftarrow 1$ and $\mathbf{X}_{m',e} \leftarrow 1$.
- 13: Reset $\mathbf{X}_{m,e} \leftarrow 0, \mathbf{X}_{m',e'} \leftarrow 0$.
- 14: **end if**
- 15: **end for**
- 16: **end while**

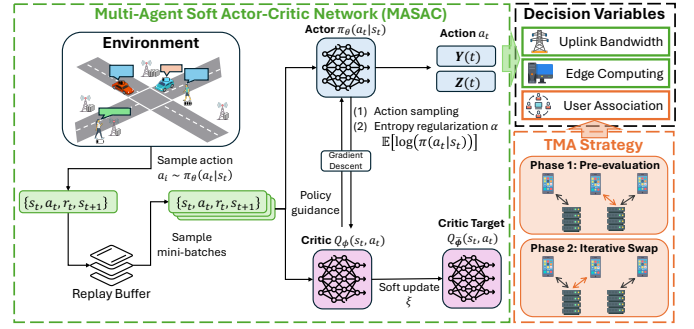


Fig. 4: Illustration of the proposed TMA-MASAC framework.

V. SIMULATION AND PERFORMANCE EVALUATION

A. Simulation Setup

TABLE I: MEC System Configurations

Parameter	Value
Target model M_p	GPT2-XL (1.6B)
Draft model M_q	GPT2 (137M)
Number of mobile devices M	30 – 180
Number of edge servers E	4 – 20
Bandwidth W (MHz)	10
Mobile transmission power P (dBm)	16 – 24
Noise power spectral density N_0 (dBm/Hz)	-174
Energy coefficient for computing δ^{CP}	10^9
Energy coefficient for communication δ^{CM}	2.6
Weight for latency synchronization λ	10^{-2}
Weight for energy consumption w	20 – 100

Simulation Configurations We model the MEC system based on the 3GPP small-cell simulation guidelines [19], with parameters detailed in Table I. The system includes a diverse set of mobile device and edge server tiers, including Samsung Galaxy S23, Apple iPhone 14, Huawei Mate 60, and NVIDIA RTX 2080, 3090 and 4090. At each time slot, each device randomly executes one of three LLM-based tasks: code generation, text summarization, or chatbot conversation. This task heterogeneity, with varying expected sequence lengths, enables effective evaluation of the system's adaptability to diverse LLM workloads.

To simulate realistic wireless environments, we use the Sionna simulator, which provides high-fidelity ray-tracing engine and stochastic channel models following 3GPP standards. Mobile devices and edge servers are positioned based on the environment geometry, and Sionna computes the channel gain \mathbf{H} , capturing path loss, multi-path fading, and user mobility.

Benchmarks We compare the proposed TMA-MASAC framework with several baseline algorithms, namely

- **Random:** Each mobile device randomly selects an edge server with uniform probability.
- **Max SINR** [20]: Each mobile device associates with the edge server offering the highest signal-to-interference-plus-noise ratio (SINR).
- **Max Compute** [21]: Each mobile device associates with the edge server offering the highest computational capacity.

B. Performance Evaluation

Figure 5 compares the latency performance of the proposed framework against baselines under varying numbers of mobile devices and edge servers. As the network scales up, our method consistently outperforms the reference schemes, achieving up to 28.0% and an average of 23.7% lower end-to-end latency. This improvement demonstrates the effectiveness of our joint UARA strategy in enabling collaborative LLM inference, even under dense and dynamic MEC conditions.

Figure 6 further examines the impact of the energy-efficiency weight w on both average latency and energy consumption across different battery levels. As w increases, a clear tradeoff emerges: energy consumption steadily decreases while latency grows, indicating that the framework successfully prioritizes energy savings over latency minimization when necessary. This effect is especially evident in low-battery devices, highlighting the framework’s responsiveness to varying power constraints. These results underscore the need for tuning w to balance latency and energy efficiency based on given system objective and device-specific conditions.

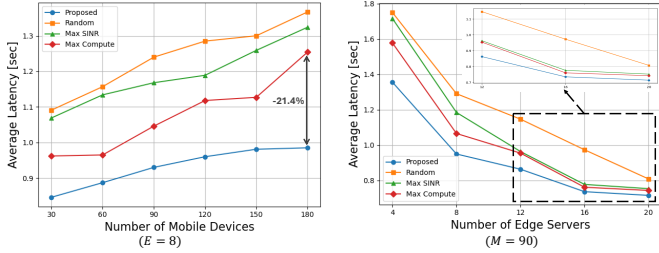


Fig. 5: Average latency under different numbers of (left) mobile devices and (right) edge servers.

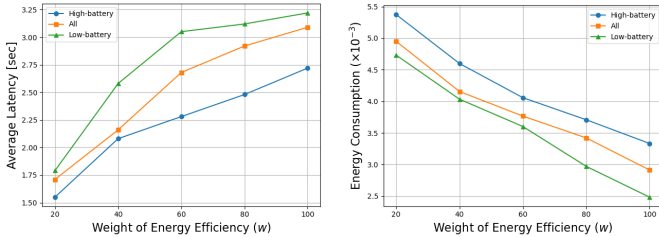


Fig. 6: Impact of energy-efficiency weight w on (left) average latency and (right) energy consumption for mobile devices with high ($B_i \geq 0.8$) and low ($B_i \leq 0.2$) battery levels.

VI. CONCLUSION

In this paper, we present a novel framework for efficient LLM inference in MEC systems by jointly optimizing UARA problem to support parallel speculative decoding. Specifically, we propose the TMA-MASAC framework, which enables synchronized collaboration between mobile devices and edge servers under dynamic resource constraints. Evaluated using the Sionna simulator, our method achieves up to 28.0% and

an average of 23.7% reduction in end-to-end latency, outperforming prior baselines. These results highlight the potential of combining parallel speculative decoding with intelligent resource management for scalable, low-latency LLM deployment in MEC settings.

REFERENCES

- [1] S. Laskaridis, K. Katevas, L. Minto, and H. Haddadi, “Mobile and edge evaluation of large language models,” in *Workshop on Efficient Systems for Foundation Models, ICML*, Jul. 2024.
- [2] K. Bin, J. Park, C. Park, S. Kim, and K. Lee, “CoActo: Coactive neural network inference offloading with fine-grained and concurrent execution,” in *Proc. Annu. Int. Conf. Mobile Syst. Appl. Services*, May 2024.
- [3] K. Huang and W. Gao, “Real-time neural network inference on extremely weak devices: agile offloading with explainable AI,” in *Proc. Annu. Int. Conf. Mobile Comput. Networking*, Oct. 2022.
- [4] Y. Leviathan, M. Kalman, and Y. Matias, “Fast inference from transformers via speculative decoding,” in *Proc. Int. Conf. Mach. Learn.*, Jul. 2023.
- [5] C. Chen, S. Borgeaud, G. Irving, J.-B. Lespiau, L. Sifre, and J. Jumper, “Accelerating large language model decoding with speculative sampling,” 2023. arXiv:2302.01318.
- [6] T. Liu, Y. Li, Q. Lv, K. Liu, J. Zhu, and W. Hu, “Parallel speculative decoding with adaptive draft length,” 2024. arXiv:2408.11850.
- [7] B. Wang, H. Kang, J. Li, G. Sun, Z. Sun, J. Wang, and D. Niyato, “UAV-assisted joint mobile edge computing and data collection via matching-enabled deep reinforcement learning,” 2025. arXiv:2502.07388.
- [8] T. Haarnoja, A. Zhou, K. Hartikainen, G. Tucker, S. Ha, J. Tan, V. Kumar, H. Zhu, A. Gupta, P. Abbeel, et al., “Soft actor-critic algorithms and applications,” 2018.
- [9] J. Hoydis, S. Cammerer, F. A. Aoudia, A. Vem, N. Binder, G. Marcus, and A. Keller, “Sionna: An open-source library for next-generation physical layer research,” 2022. arXiv:2203.11854.
- [10] W. Zhao, Y. Huang, X. Han, C. Xiao, Z. Liu, and M. Sun, “Ouroboros: Speculative decoding with large model enhanced drafting,” 2024. arXiv:2402.13720.
- [11] T. Cai, Y. Li, Z. Geng, H. Peng, J. D. Lee, D. Chen, and T. Dao, “Medusa: Simple llm inference acceleration framework with multiple decoding heads,” 2024. arXiv:2401.10774.
- [12] Y. Fu, P. Bailis, I. Stoica, and H. Zhang, “Break the sequential dependency of llm inference using lookahead decoding,” 2024.
- [13] Y. Zhou, K. Lyu, A. S. Rawat, A. K. Menon, A. Rostamizadeh, S. Kumar, J.-F. Kagy, and R. Agarwal, “DistillSpec: Improving speculative decoding via knowledge distillation,” 2023.
- [14] X. Miao, G. Oliaro, Z. Zhang, X. Cheng, Z. Wang, Z. Zhang, R. Y. Y. Wong, A. Zhu, L. Yang, X. Shi, et al., “Specinfer: Accelerating large language model serving with tree-based speculative inference and verification,” in *Proc. ACM Int. Conf. Archit. Support Program. Lang. Operating Syst.*, vol. 3, pp. 932–949, 2024.
- [15] Z. Hao, H. Jiang, S. Jiang, J. Ren, and T. Cao, “Hybrid SLM and LLM for edge-cloud collaborative inference,” in *Workshop on Edge and Mobile Foundation Models, EdgeFM*, Jun. 2024.
- [16] H. Jin and Y. Wu, “CE-CoLLM: Efficient and adaptive large language models through cloud-edge collaboration,” 2024. arXiv:2411.02829.
- [17] M. Kim, J. Jang, Y. Choi, and H. J. Yang, “Distributed task offloading and resource allocation for latency minimization in mobile edge computing networks,” *IEEE Trans. on Mobile Comput.*, vol. 23, pp. 15149–15166, 2024.
- [18] Y. Deng, Z. Chen, X. Chen, and Y. Fang, “Throughput maximization for multi-edge multiuser edge computing systems,” *IEEE Internet Things J.*, vol. 9, pp. 68–79, 2021.
- [19] 3GPP, “NR: physical layer procedures for data,” Jul. 2020.
- [20] T. Liu, S. Ni, X. Li, Y. Zhu, L. Kong, and Y. Yang, “Deep reinforcement learning based approach for online service placement and computation resource allocation in edge computing,” *IEEE Trans. Mobile Comput.*, vol. 22, pp. 3870–3881, 2022.
- [21] X. Ma, A. Zhou, S. Zhang, Q. Li, A. X. Liu, and S. Wang, “Dynamic task scheduling in cloud-assisted mobile edge computing,” *IEEE Trans. Mobile Comput.*, vol. 22, pp. 2116–2130, 2021.